Solid State Science and Technology, Vol. 25, No 2 (2017) 134-144
ISSN 0128-7389 | *http://journal.masshp.net*

PREPARATION AND CHARACTERIZATION OF HEMATITE (Fe_2O_3) - HALLOYSITE NANOTUBES (HNTs) NANOCOMPOSITES

Shafinas Abdullah[1] and Mohamad Abu Bakar[2]

[1]*Faculty of Applied Sciences, Universiti Teknologi MARA, Tapah Campus, Tapah Road, 35400, Perak, Malaysia*

[2]*School of Chemical Sciences, Universiti Sains Malaysia, 11800 USM Pulau Pinang, Malaysia*

Corresponding author: shafinas@perak.uitm.edu.my

ABSTRACT

Hematite (Fe_2O_3)-halloysite nanotubes (HNTs) nanocomposites were successfully synthesized via self-assembly of hematite (Fe_2O_3) nanoparticles and halloysite nanotubes (HNTs) building blocks. The nanocomposites were prepared via Polyvinyl Alcohol (PVA) routes. The as-prepared hematite/HNTs nanocomposites had been characterized by Transmission Electron Microscopy (TEM), Scanning Electron Microscopy (SEM), Fourier Transform Infrared (FTIR), X-ray Diffraction (XRD), and Electrical Impedance Spectroscopy (EIS). The analysis of the results, indicates that the samples prepared via PVA routes with ferric nitrate nanohydrate [$Fe(NO_3)_3.9H_2O$] shows better result in size distribution of nanoparticles. Other than that, based on the analysis of electrical impedance spectroscopy (EIS) measurement, the use of PVA as capping agent in the preparation of hematite/HNTs nanocomposites improved the conductivity properties.

Keywords: hematite; halloysite nanotubes; hematite/halloysite nanotubes nanocomposites

INTRODUCTION

Nowadays, terms like nanomaterials, nanocomposites, nanosystems, and nanostructures become important to many technologies [1]. There is an extensive worldwide effort in order to introduce nanotechnology for the production of materials with specific functional characteristics such as semiconducting, electromagnetic, optical, and else. In short, there is a great potential for the wide use of nanotechnology for functional materials and devices [2].

Nanostructures such as nanotubes and nanospirals of clay minerals are very versatile systems, and are target materials for many applications [3]. In recent years, halloysite nanotubes (HNT) has regained attention due to a rise interest in tube-like nanoparticles in materials science and technology. It is a clay mineral describes as a gibbsite

octahedral sheet ($Al(OH)_3$), which is modified by siloxane groups at the outer surface, and has a 1:1 of Al:Si ratio and stoichiometry $Al_2Si_2O_5(OH)_4.nH_2O$ [3,4]. Some advantages using halloysite nanotubes are it is naturally occuring clay, non-toxic, biocompatible, fine particle size, high surface area, good dispersion, fast adsorption rate, high adsorption capacity, and more cheaper compared to other clay [5].

In order to enhance the conductivity properties, HNTs must be coated with metallic and other substances to achieve a wide variety of electrical, chemical, and physical properties. The hollow tube of HNTs can be filled with a variety of active ingredients such as metals. In this study, we had reported the preparation and characterization of hematite/HNTs nanocomposites. The influences and distribution of hematite in halloysite nanotubes had been studied.

EXPERIMENTAL

Material

The following chemicals were commercially available and were used without further purification; Polyvinyl Alcohol (PVA) (Sigma-Aldrich, Germany), Ferric Nitrate Nanohydrate [$Fe(NO_3)_3.9H_2O$] (Sigma-Aldrich, USA), and Halloysite nanoclay (HNTs) (Aldrich, USA).

Preparation of Fe_2O_3/HNTs using PVA routes

The raw material used were $Fe(NO_3)_3.9H_2O$, PVA, and HNTs. The chemicals were stoichiometrically weighed and dissolved in a minimum quantity of distilled water. A certain amount of ferric nitrate solution was added into 40 mL of 10 wt. % aqueous solution of PVA. For 1:5 mole ratio of metal ion and PVA, an amount of 0.8045 g of ferric nitrate nanohydrate and 4.0020 g of PVA was used. After that, 0.8004 g HNTs was added into the solution mixture and stirred at 60 – 70 ºC for 12 hours. In order to ascertain the HNTs to expand, the solution was further stirred for another 12 hours at room temperature and then followed by sonication for 10 minutes. Next, the solvent used which is distilled water in this preparation was allowed to evaporate by heating at 100 ºC for 3 hours. The residue left was then calcined at 400 ºC for 2 hours. The calcined sample was ground well for further analysis. The preparation of hematite/HNTs nanocomposite was repeated by using different mole ratio of metal ion:PVA such as 1:3 and 1:2. For mole ratio of 1:3, an amount of 1.3288 g ferric nitrate nanohydrate, 4.0014 g of PVA and 0.8006 g HNTs were used. For the sample with a 1:2 mole ratio, the respective amount of ferric nitrate nanohydrate, PVA and HNTs used were 2.0428 g , 4.0003 g and 0.8000 g.

Characterization

Philips CM12 transmission electron microscope (TEM) (Netherlands) with 80 kV accelerating voltage was used to determine the morphology, dispersion, and distribution of particles in nanocomposites. The powder samples were generally prepared by suspension in ethanol. The suspension was dropped onto a carbon-coated copper grids and then allowed to dry in air for direct observation. Scanning Electron Microscopy

(SEM) was used to analyze the filler dispersion and surface morphology of the prepared hematite/HNTs nanocomposites in the form of powder using Quanta-FEG 650 (Holand). The samples were sputter coated with thin layer of chromium in order to avoid the artifacts associated with sample charging during experiments and to make the sample conductive. Operating condition voltage 5 kV, probe current 45 nA, and counting time 60 seconds were used. Perkin Elmer System 2000 Fourier Transform Infrared (FTIR) spectrophotometer (USA) was used to determine the chemical functional groups present in the samples. The sample preparation method used involves mixing the finely ground sample with powdered potassium bromide and pressing the mixture under high pressure. The results is a KBr pellet that can be inserted into a holder in the spectrometer. The spectra were recorded in the mid-infrared range of 4000 – 400 cm^{-1} at room temperature. The crystalline phases of pristine HNT_S, pristine hematite anda hematite/HNTs nanocomposites were identified by X-Ray Diffraction (XRD) analysis using Phillips X'Pert (USA) D/max – 2550VB + 18-kW powder diffractometer with Cu kα radiation (λ = 1.5418 Å). The data were collected in the scanning range 2θ = 20 – 80º, with a scanning speed of 2º min^{-1}. The conductivity properties of the pristine HNTs and hematite/HNTs nanocomposites were analyzed using Electrical Impedance Spectroscopy (EIS). This analysis was performed by a GAMRY instruments framework response analyzer coupled with a potentiostat, both interfaced with a personal computer. The analyses were run with only two electrode system instead of the classic three electrode system ignoring the reference electrode to the system. This is due to the sample in solid form. Both electrodes used are stainless steel. The impedance data were analyzed by Echem Analyst program. All powder samples were made into disc as KBr-FTIR disc shape.

RESULTS AND DISCUSSION

TEM Analysis

Figure 1 shows the TEM micrograph of pristine HNTs and its representatives nanocomposites containing hematite, Fe_2O_3. Figure 1(a) shows the morphologies of white pristine HNTs with cylindrical hollow tubes averaging of 516 nm in length with an external diameter of 68 nm and internal diameter of 14 nm. After the assembly with hematite nanoparticles, the characteristics tube morphology of the pristine HNTs has been taken (Figure 1(b)). It can be proven from the figure that hematite nanoparticles are densely dispersed on the external and internal surfaces of HNTs. The average size of hematite nanoparticles for hematite/HNTs nanocomposites prepared using PVA is 10 nm. Some hematite nanoparticles were found to attach on the wall of the hollow cavities of HNTs as marked in Figure 1 (b). From previous study by Xie *et al*., it was stated that the attachment on the surface of HNTs could be related to the structures of HNTs, it has large surface area, large pore volume and adequate hydroxyl groups, which allowed the metal ions to be attached and adsorbed on the surface of HNTs easily [6]. Furthermore, from the result obtained, sample preparation via PVA routes with ferric nitrate nanohydrate shows better result which is size of nanoparticles much uniform due to PVA can attach the metal colloidal more easily. This is in agreement with David *et al.,*

who reported that PVA can react with metal salts in an aqueous solution to form metal chelate [7]. Patil and Joshi also stated that PVA added to metal salt can acts both as an encapsulating and complexing agent. It also helps in the habitual modification size of hematite particles [8].

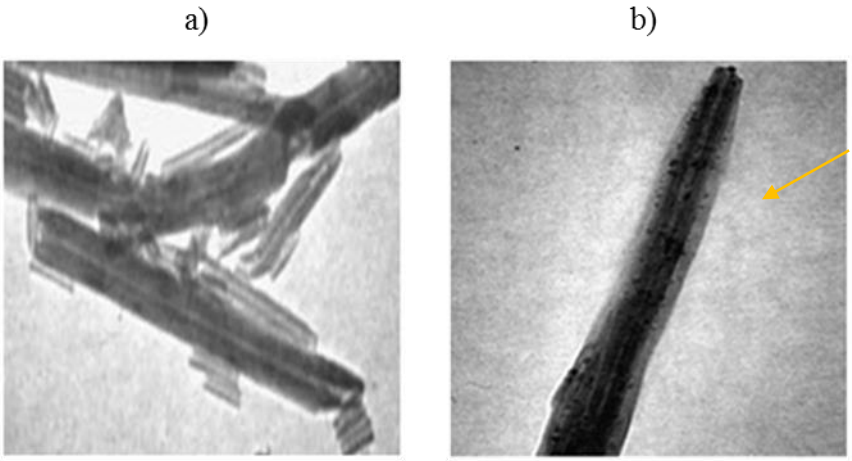

Figure 1: TEM micrographs of (a) pristine HNTs, (b) PVA-Fe_2O_3-HNTs

Surface morphology

The chemical composition and morphology of HNTs and its representatives nanocomposites containing hematite were measured through SEM-EDX. As shown in Figure 2, some hematite nanoparticles agglomerated on the fractured surfaces of the hematite/HNTs nanocomposites. Besides, SEM morphology shows that the size distribution of hematite/HNTs nanocomposites using PVA are less agglomerate. This is might due to the carbon network presence in PVA which can effectively prevent the agglomeration of hematite nanoparticles [8]. The EDX spectra on Figure 2 confirmed the presence of hematite nanoparticles. The well-dispersed hematite nanoparticles were mainly deposited on the external surface of the HNTs. The EDX spectra proved that the major constituents for HNTs were Al, Si, and O and the peaks of Al, Si and O were mainly generated by HNTs. From the morphology of hematite/HNTs nanocomposites, the hematite nanoparticles were irregularly dispersed on the surface of HNTs which causes the surface of hematite/HNTs to become rough [9].

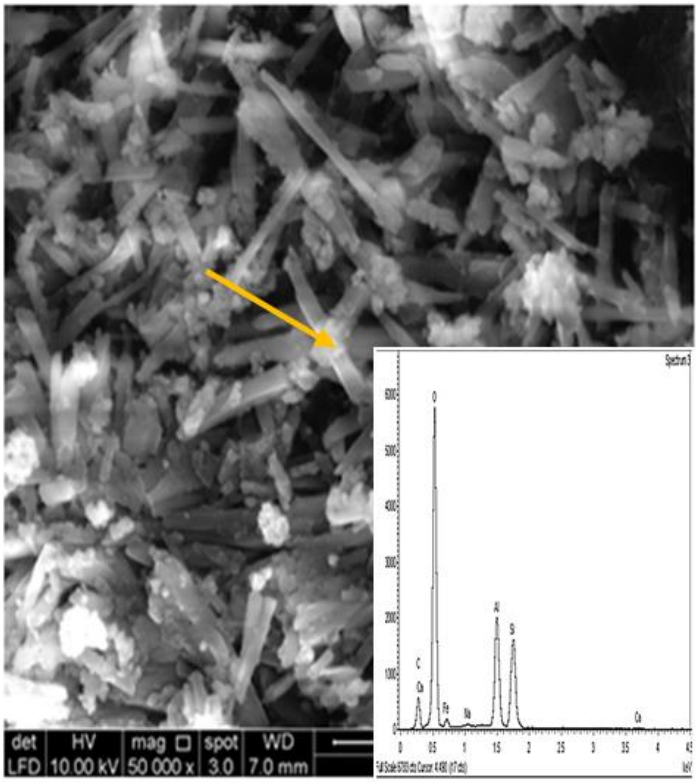

Figure 2: SEM micrograph and SEM-EDX at 50000 magnification of PVA-Fe_2O_3-HNTs

FTIR Spectra

Figure 3(i) shows the FTIR spectrum of pristine Halloysite Nanotubes (HNTs). As can be seen, the peak at 3694 cm^{-1} can indicates the presence of -OH stretching vibration of the inner-surface of Al-OH groups. The peak at 3621 cm^{-1} can be related to the -OH stretching vibration of the inner Al-OH groups which is between the interface of the Si-O tetrahedron and the Al-O octahedron. The broad peak between 1638 and 3437 cm^{-1} arises from adsorbed water. The peak at 1030 cm^{-1} corresponds to the in-plane stretching vibration of the Si-O network such as Si-O-Si and O-Si-O. The peak at 912 and 536 cm^{-1} indicate the presence of O-H deformation vibration of inner Al-OH groups and deformation vibration of Al-O-Si and also Al-O tetrahedral sheets respectively. The Si-O-Si deformation vibration observed at 469 cm^{-1} is attributed to Si-O tetrahedral sheets [10].

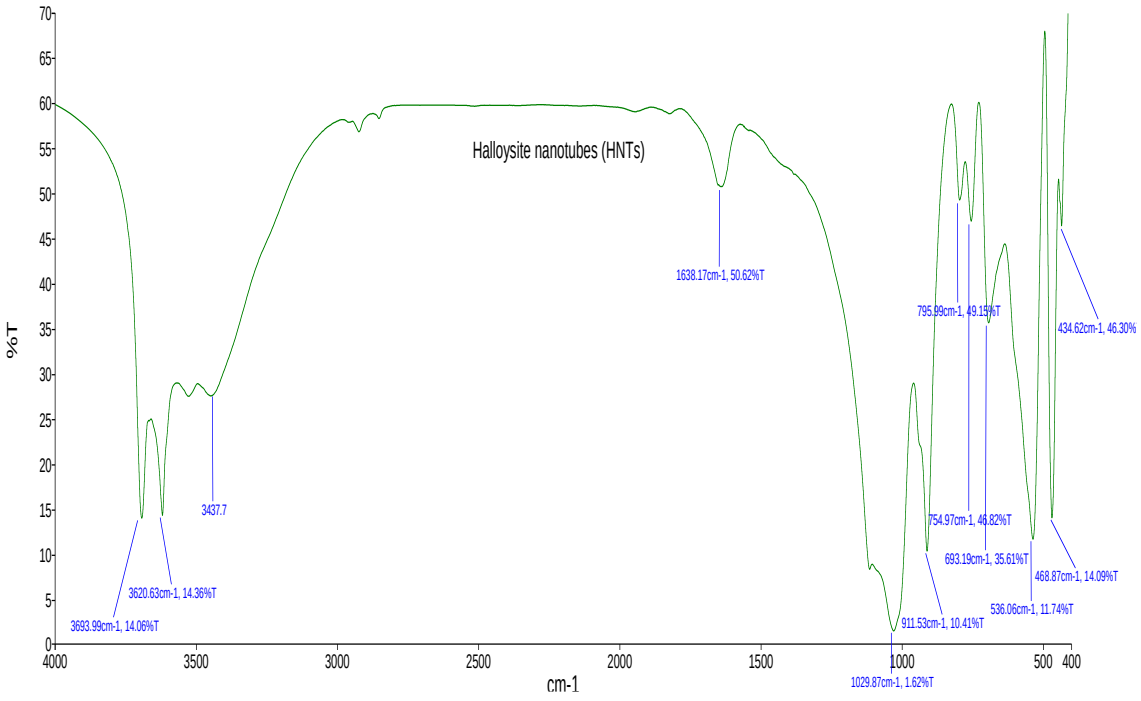

Figure 3: (i) FTIR Spectrum of pristine HNTs

Figure 3(ii) shows the FTIR spectra of representatives nanocomposites containing hematite via thermal decomposition using PVA. The FTIR spectra of hematite/HNTs nanocomposites show characteristics peak of both hematite and HNTs. The broad band around 3430 cm^{-1} observed as compared to pristine HNTs due to the presence of stretching vibration of hydroxyl group of hematite. The band of Al-O-Si of HNTs at below 600 cm^{-1} and the hematite characteristic peak at around 580 cm^{-1} could be overlapped in hematite/HNTs nanocomposites. The intensity of the peak of hematite/HNTs nanocomposites Si-O network around 1032 cm^{-1} much lower as compared to the peak of pristine HNTs. This might be due to hematite/HNTs, associated with the formation of bond between hematite and HNTs [6]. Besides, in the presence of PVA, hydrogen bonding was produced. It can be proved by the peak of adsorbed water around 3455 and 1611 cm^{-1} for samples using PVA show shifted and broadened in peak.

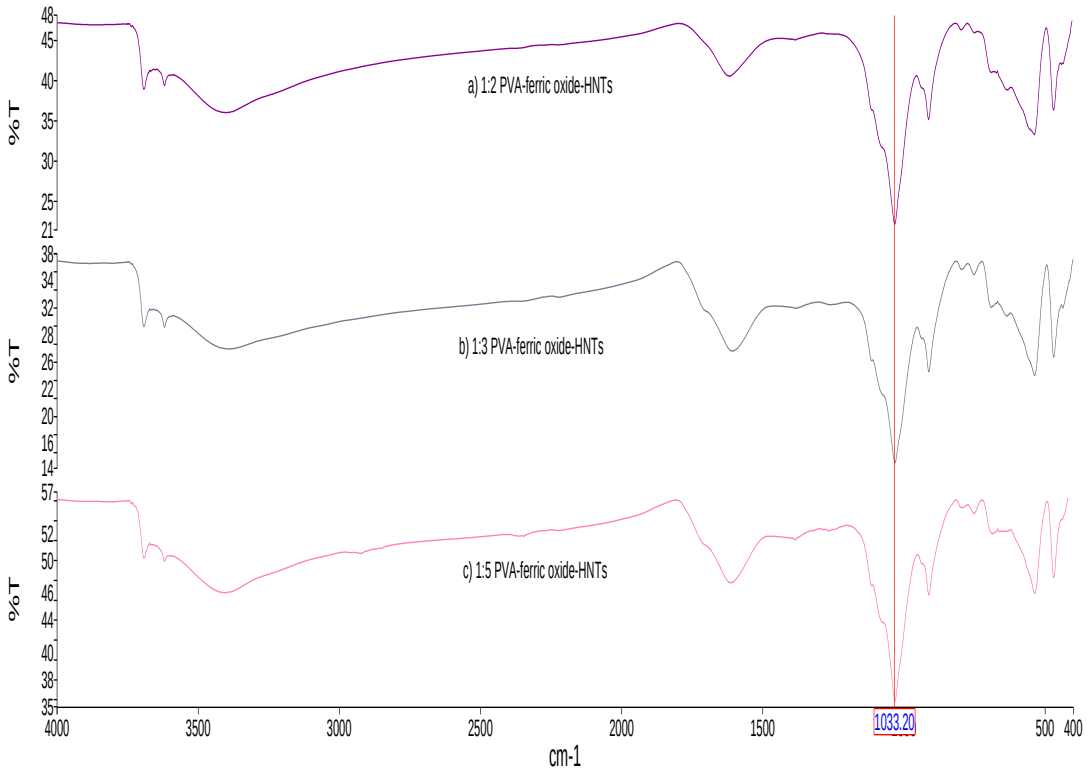

Figure 3 (ii) FTIR spectrum of (a) 1:2 PVA-Fe_2O_3-HNTs, (b) 1:3 PVA-Fe_2O_3-HNTs, and (c) 1:5 PVA-Fe_2O_3-HNTs

XRD Analysis

Figure 4 shows the XRD pattern of pristine HNTs, pristine hematite and PVA-Fe_2O_3-HNTs. For the pristine HNTs and hematite samples, all of the observed peaks are closed to the characteristics data of halloysite and hematite (JCPDS card No. 00-009-0453) and (JCPDS card No. 01-089-0596) respectively. The dominant phase of pristine HNTs was at $2\theta = 11.94°$, 20.43°, 24.56°, and 26.55° with hkl plane d(001), d(100), d(002), and d(003) respectively while at $2\theta = 35.60°$ and 62.44° are due to hematite dominant phase. d(110) and d(214) matched well with the hematite/HNTs nanocomposites prepared. The pristine HNTs show a diffraction peak at $2\theta = 11.94°$ with d spacing of 7.41 Å which is related to d(001) plane. This basal reflection of HNTs is due to its tubular morphology, high degree of disorder, small crystal size and interstratifications of layer with various hydration states [11]. This peak of HNTs in the PVA-Fe_2O_3-HNTs nanocomposite is shifted to a higher 2θ value as compared to the pristine HNTs. The d-spacing of PVA-Fe_2O_3-HNTs nanocomposite are 7.21 Å at 2θ of 12.26°. The reduction of basal spacing and increasing of the 2θ of the HNTs may be attributed to the de-intercalation of the HNTs [12]. This might be due to the nanotube like of HNTs. In the XRD pattern of hematite/HNTs nanocomposites, both hematite and HNTs diffraction peaks were observed. As compared with the pristine HNTs and hematite, diffraction peaks of representative nanocomposites are weaker, which may be attributed to their lower amount in the nanocomposites. Besides, no characteristics peak of bulk hematite was observed in the hematite/HNTs nanocomposites which indicate that hematite have

been dispersed in micropores of the HNTs clay [11].

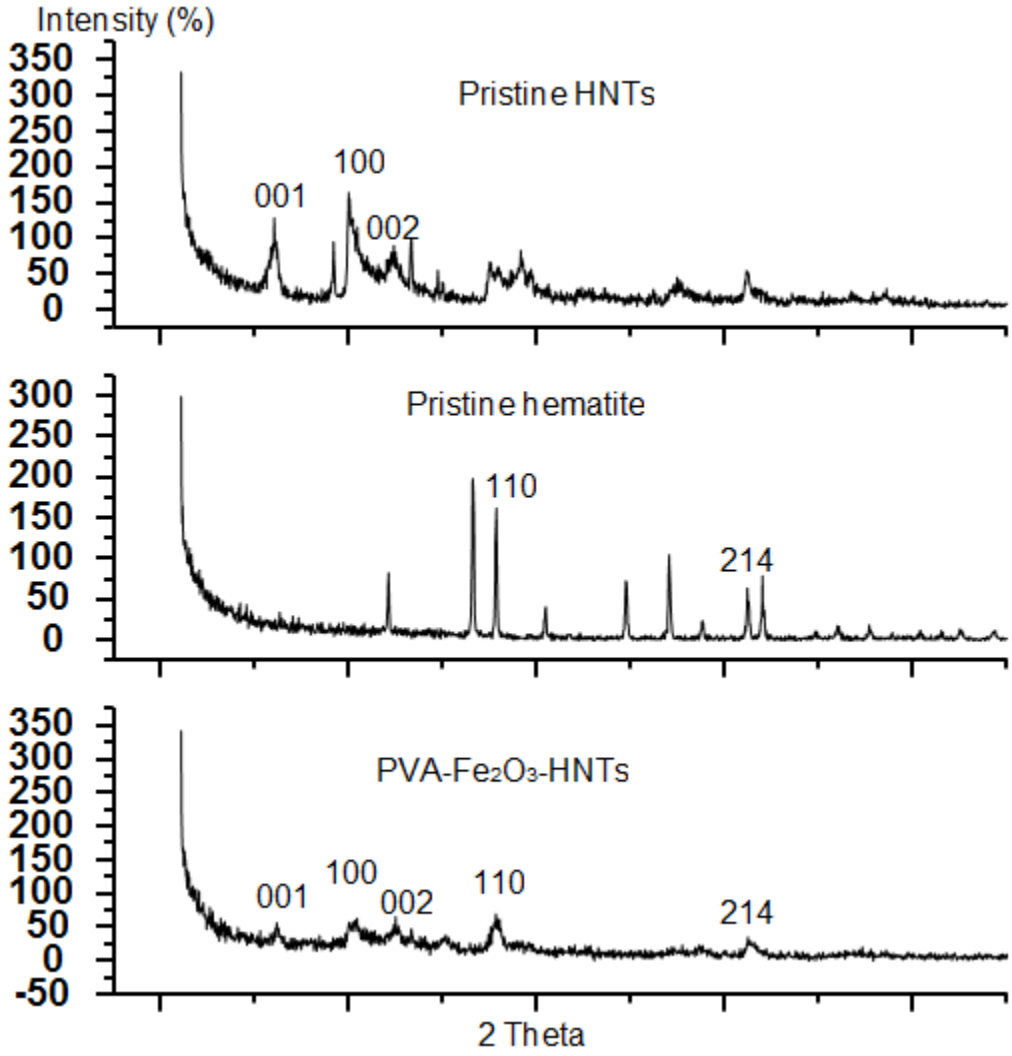

Figure 4: XRD patterns of (a) pristine HNTs, (b) pristine hematite, and (c) PVA-Fe_2O_3-HNTs

Impedance Analysis

In impedance analysis, resistivity which is simply the inverse of the conductivity, was measured because the multimeter only shows resistance value [13]. From the Nyquist plot in Figure 5(a), it can be observed that HNTs is not a conducting material due to its high resistance. As compared to Figure 5(b), the presence of hematite nanoparticles increase the conductivity properties of HNTs. This might be due to the presence of PVA which enhances the nanocomposite properties. The conductivity of the pristine HNTs and its representatives nanocomposites containing hematite was calculated according to the formula below based on ASTM Standard D257 [14]. The results of conductivity and resistance of pristine HNTs and its representatives are tabulated in Table 1.

$$conductivity\ material, \sigma = \frac{L\ (cm)}{Resistance\ (\Omega) x\ Area\ (cm^2)}$$

(a)

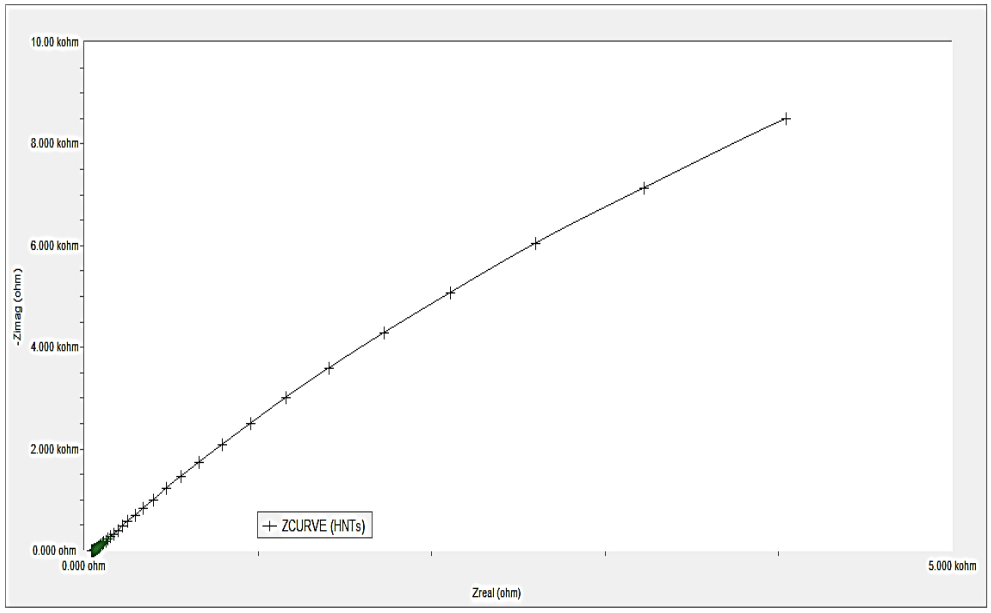

(b)

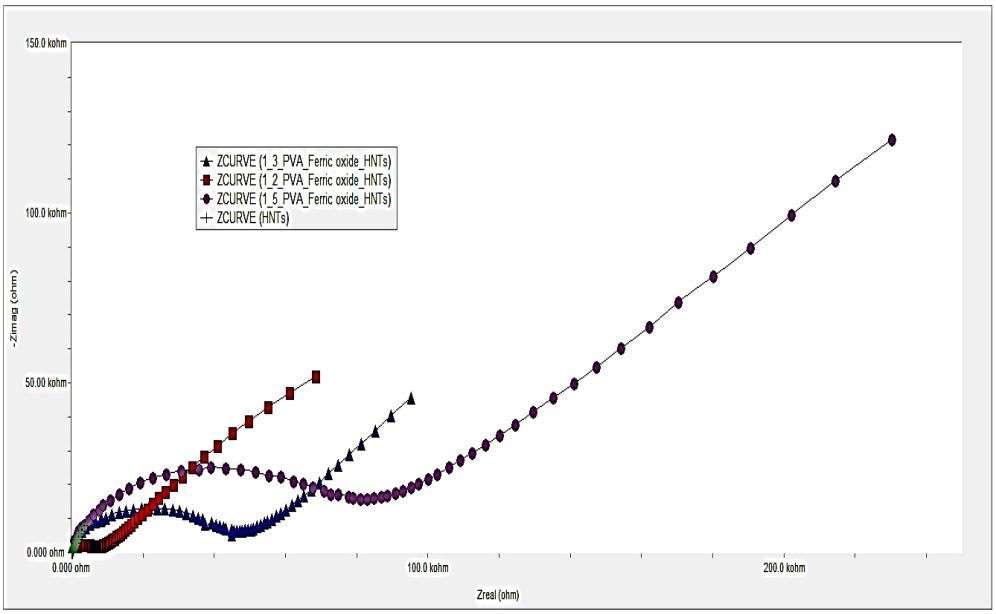

Figure: 5 Nyquist plot of (a) pristine HNTs, (b) PVA-Fe_2O_3-HNTs

Table 1: The conductivity and resistance of pristine HNTs and its representative nanocomposites

Samples	Resistance, Ω	Conductivity, Ω^{-1}/cm
Pristine HNTs	4.82×10^{5}	3.50×10^{-8}
1:2 PVA-Fe_2O_3-HNTs	1.09×10^{4}	2.00×10^{-6}
1:3 PVA-Fe_2O_3-HNTs	7.72×10^{4}	2.83×10^{-7}
1:5 PVA-Fe_2O_3-HNTs	1.08×10^{5}	2.02×10^{-7}

CONCLUSIONS

Hematite/HNTs nanocomposites has been successfully synthesized using self-assembly of hematite nanoparticles and halloysite nanotubes (HNTs) via PVA routes. The crystalline phase , surface morphology, and the effect of interaction between hematite nanoparticles on HNTs has been successfully investigated. The conductivity properties of hematite/HNTs nanocomposites improved when capped with PVA.

REFERENCES

[1] Utracki, L. A. (n.d.). *Clay-Containing Polymeric Nanocomposites* (Vol. 1). Smithers Rapra Technology, United Kingdom.

[2] Rahman, M. M., Khan, S. B., Jamal, A., Faisal, M., and Aisiri, A. M. (n.d.). Iron Oxide Nanoparticles.

[3] Duarte, H. A., Lourenço, M. P., Heine, T., and Guimarães, L., Clay Mineral Nanotubes: Stability, Structure and Properties, Chapter 2, Stoichiometry and Materials Science – When Numbers Matter¸ InTech, 2012

[4] Guimaraes, L., Enyashin, A.N., Seifert, G. and Duarte, H.A. *Journal of Physical Chemistry C,* **114** 11358-11363 (2010)

[5] Joussein, E., Petit, S., Churchman, J., Theng, B., Righi, D. and Delvaux, B. *Clay Minerals* **40** 383-426 (2005)

[6] Xie, Y., Qian, D., Wu, D., and Ma, X. *Chemical Engineering Journal*, **168** (2) 959–963 (2011)

[7] David, L., Espuche, E., and Lyon, D. (2007). Structure and Morphology of Nanocomposite Films Prepared from Polyvinyl Alcohol and Silver Nitrate : Influence of Thermal Treatment, *Wiley InterScience*, 2657–2672

[8] Patil, P. R., and Joshi, S. S. *Metal-Organic, and Nano-Metal Chemistry*, **37** (6) 425–429 (2007)

[9] Xing, W., Ni, L., Huo, P., Lu, Z., Liu, X., Luo, Y., and Yan, Y. *Applied Surface Science*, 259, 698–704 (2012)

[10] Zhang, Y., He, X., Ouyang, J., and Yang, H. *Scientific Reports*, **3** (29) 2948

(2013)
[11] Rooj, S., Das, A., Thakur, V., Mahaling, R. N., Bhowmick, A. K., and Heinrich, G. *Materials & Design*, **31** (4) 2151–2156 (2010)
[12] Ismail, H., Pasbakhsh, P., Fauzi, M. N. A., and Bakar, A. A. *Polymer Testing*, **27** 841–850 (2008)
[13] Ghani, S. A., and Young, H. C. *Journal of Physical Sciences*, **21** (2) 81–97 (2010)
[14] Kulshreshtha, A. K. (2002). Handbook of polymer blends and composites, 1st ed., vol. 2. UK: Rapra Technology Limited